International Journal of Engineering Research and Development
e- ISSN: 2278-067X, p-ISSN: 2278-800X, www.ijerd.com
Volume 21, Issue 6 (June 2025), PP 102-109

Mn^{2+} Doped K_2SO_4 Single Crystal's Local Structure and Optical Absorption

Maroj Bharati [a], Vikram Singh [a], Ram Kripal [b]
[a] *Department of Physics, Nehru Gram Bharti (DU), Jamunipur, Prayagraj, India*
[b] *EPR Laboratory, Department of Physics, University of Allahabad, Prayagraj-211002, India*

Abstract
Employing perturbation theory and the superposition model, the splitting parameters for the zero field of Mn^{2+} doped crystals of K_2SO_4 are obtained. When the local distortion is included in the computation, the determined parameters fairly match the experimental ones. Theoretical evidence corroborates the experimental finding that the Mn2+ ion substitutes at the K^+ site in K_2SO_4. The optical spectra of the system are computed by diagonalizing the complete Hamiltonian in the coupling scheme of the intermediate crystal field, using the crystal field parameters obtained from the superposition model and the crystal field analysis program. The calculated and experimental band locations agree fairly well. Consequently, the results of the experiment are confirmed by the theoretical analysis.
Keywords: *Inorganic compounds, Single crystal, Crystal fields, Electron paramagnetic resonance, Zero field splitting.*

Date of Submission: 06-06-2025 Date of acceptance: 16-06-2025

I. Introduction

The method of electron paramagnetic resonance (EPR) can be used to ascertain the transition metal ions' energies as they go through Zeeman transitions. Mn^{2+} ion is the most studied transition ion since, even at room temperature, it emits the EPR signal. This ion has $3d^5$ electronic configuration and its ground state is $^6S_{5/2}$. The paramagentism of this ion can be attributed to only the electron spin because the ion has zero angular momentum. The small structural changes of the crystal [1-3] show sensitiveness to the zero field splitting of this ion in crystals.

For use in EPR [4-6] and optical spectroscopy [7-8], the parameters for zero field splitting (ZFS) and crystal field (CF) can be semi-empirically modeled using the superposition model (SPM). In [9], the spin Hamiltonian (SH) along with other Hamiltonians is discussed. The parameters of the crystal field (CF) are often found utilizing SPM and the point-charge model [10] even if the exchange charge model (ECM) is a useful technique as well for analysing the effects of crystal fields in single crystals incorporated with rare earth and transition ions [11]. In this study, we used SPM to calculate the ZFS parameters and the CF parameters. SPM was suggested [12] for CF based on the assumptions: (1) An algebraic total of the crystal's other ions' contributions can be used to determine the paramagnetic ion's CF. All the significant contributions to the conservation of free energy from each paramagnetic ion have axial symmetry with respect to their position vector when the ion is in the chosen coordinate system's origin. (3) The CF contributions of just nearby or coordinated ions are to be taken into account. (4) Across various host crystals, contributions to CF from a solitary ion (ligand) can be transmitted. The axial symmetry assumption, however (2) permits the transformation of one coordinate system into another, the first assumption provides support for the applicability of superposition principle in characterising the CF. Nonetheless, a more limited version of assumption (3) is sometimes utilised, when solely the closest neighbour ions are occupied. According to the final ligand transferability assumption (4), the only factors influencing the contributions of one ion to CF are its character and separation from the paramagnetic ion. In order to perform an SPM analysis on the CF, it is essential to obtain a stable polar coordinate system (R_L, θ_L, Φ_L) for each ligand or ion from the host crystal's X-ray data. When transition metal ions are doped, ionic size, ionic charge, and inter-ionic bonding mismatches will probably result in some degree of local distortion. To find the fitted values of the SPM power-law exponents and the intrinsic parameters, a non-linear or linear least-square fit may be performed on an adequate quantity of CF parameters. Mn^{2+} and Fe^{3+} experimental spin-Hamiltonian parameters in CaO and MgO crystals have been critically analysed [13]. For the EPR data, it gives the SPM parameters' exact values and demonstrates that the superposition principle is satisfied by the CF for 3d ions. A strict lattice relaxation model was utilised [14] to ascertain sets of SPM intrinsic parameters based on dependable ligand distances for the oxides of alkali earth.

For Fe^{3+} and Mn^{2+} doped MgO, CaO, and SrO (R0 = 2.0 Å): $\overline{b_2}$ = (-1552±48) $\times 10^{-4}$ cm^{-1} and (-6440±113) $\times 10^{-4}$ cm^{-1}, respectively, with a fixed t_2 = 16 for both ions. For both Fe^{3+} and Mn^{2+}, the values of $\overline{b_4}$ are 9.9±0.8 $\times 10^{-4}$ cm^{-1}, with a fixed t_4 of 16±4 for each ion. The fitted values for Mn^{2+} and Fe^{3+}, respectively, were 17.7 and 14.4 for the separate fitting of t_2.

Potassium Sulfate (PS) is an inorganic compound with the chemical formula K_2SO_4. As a chemical compound, it is observed to be odorless, hard, and has a saline like- taste. Potassium sulfate is orthorhombic D_{2h}^{16} at room temperature; when the temperature is higher than 583 ℃, it gradually transforms into trigonal D_{3d}^{3}. Potassium sulfate is mainly used as fertilizer and applied to some chlorine-avoiding crops like tobacco, citrus, grapes, tea, flax, potatoes, vegetables, etc. Potassium sulfate is also an important chemical raw material, which can be used to prepare potassium alum, potassium water glass, potassium carbonate and potassium persulfate, etc. It is also used as a drug (slow release agent). It is a component of gunpowder that is used in artillery and acts as a flash suppressant. Potassium sulfate is used in making lubricants and dyes and because it is hard and soluble in water, as a substitute for soda in soda blasting. It is used in animal feed and in pyrotechnics for creating a purple flame [15]. The natural sources of Potassium Sulfate are minerals like Kainite, Schonite, Leonite, Langbeinite, Polyhalite, and Aphthitalite [16]. Single crystals of undoped potassium sulfate and those doped with Mg^{2+}, Zn^{2+}, Cu^{2+}, and Mn^{2+} ions have had their electrical conductivity measured. The lower symmetry of K_2SO_4 is responsible for the lower defect formation energy in comparison to high symmetry cubic systems, while the presence of divalent ions raises the cation migration energy.

Over a temperature range of 300–145 K, a detailed EPR study of the Mn^{2+} ion in single crystals of K_2SO_4 has been conducted [17]. It is proposed to replace β-K^+ with Mn^{2+}, which is linked to β-K^+ vacancies that are first-, second-, and third-neighbor related. Analysis and reporting of parameters have been done for the room temperature spectra. A probable phase change is indicated by the studied variation in the fine-structure spread with temperature, which is around 143K (-130°C).

In the current study, the ZFS parameters D and E are calculated for the Mn^{2+} ion in PS at substitutional β-K^+ site at 300 K using CF parameters estimated from SPM and perturbation equations [18]. The aim is to find the location of Mn^{2+} ion and the distortion taking place in the crystal. The results found for the Mn^{2+} ion at substitutional β-K^+ site in PS crystal with local distortion yield reasonable match with the experimental values. Additional objective of the study seeks to obtain the extent to which CF theory and SPM analysis can be applied to Mn^{2+} ions in PS crystals in order to create an SPM parameter database. Molecular nanomagnet (MNM) design and computer modeling of their magnetic and spectroscopic characteristics will be determined by this. SMMs, or single-molecule magnets, [19], single-chain magnets (SCM) [20], and single ion magnets (SIM) [21] are currently included in the transition ion-based MNM class. The above systems have drawn large attention because of the noteworthy magnetic characteristics of MNM, for instance, magnetization's macroscopic quantum tunneling and potential uses in quantum computing and high-density information storage [19, 20]. There have been numerous synthesized SCM or SMM systems with $Mn^{2+}$and Cr^{3+} ions [22]. The parameters of the model established in this case may be used for ZFS parameter calculations for Mn^{2+} ions at similar sites in MNM, since model calculations for simpler crystal systems can serve as a foundation for more complex ones. The modeling employed in this work can be extended to explore crystals of scientific and industrial interest in numerous other ion-host systems.

II. Crystal Structure

Detailed structure of K_2SO_4 was determined by Ogg [23]. The atoms of sulfur are arranged on reflection planes, which are the SO_4 group's symmetry planes. The SO_4 group has two oxygen atoms on the plane and the other two equally spaced from it. Layers of atoms spaced a/2 apart and parallel to (100) make up the structure. The coordinate origin, denoted by the center of the unit, is the reflection planes $(100)_{1/4}$ and $(100)_{-1/4}$. The K^+ ions in the crystal are divided into two groups, designated as α and β. For the two sets of potassium ions in the structure, there are differences in their oxygen environments. The dimensions of unit cell at room temperature are 5.731 Å for *a*, 10.008 Å for *b*, and 7.424 Å for *c*. At room temperature, the crystal's symmetry is orthorhombic, and its space group is D_{2h}^{16} [23]. The crystal structure of potassium sulfate with symmetry adopted axis system (SAAS) is depicted in Fig. 1.

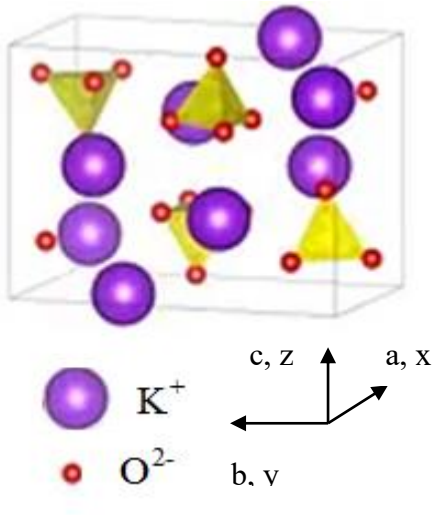

Fig. 1. K_2SO_4 crystal structure with symmetry-adopted axis system (SAAS) at 300 K.

III. Crystal Field and Zero Field Splitting Parameter Calculations

The analysis of EPR spectra is done with the spin Hamiltonian [5]:

$$\mu_B B.g.S + D\left\{S_Z^2 - \frac{1}{3}S(S+1)\right\} + E(S_x^2 - S_y^2) = \mathcal{H} \qquad (1)$$

where B, μ_B, g, D and E are the applied magnetic field, Bohr magneton, splitting factor, second rank axial, and second rank rhombic ZFS parameters [24–25]. The a, b, and c crystal axes are along the laboratory axes (x, y, z). The directions of metal-ligand bonds that are mutually perpendicular are referred to as the local symmetry axes of the site or the symmetry adopted axes (SAA). As demonstrated in Fig.1, the axis-Z of SAAS is along the crystal axis- c, and (X, Y) are perpendicular to the axis-Z. When Mn^{2+} ions are doped in K_2SO_4 crystal, these enter the lattice at substitutional β-K^+ sites with some local distortion [26].

For a $3d^5$ ion, the spin Hamiltonian can be written as [27],

$$\mathcal{H} = \mathcal{H}_o + \mathcal{H}_{so} + \mathcal{H}_{ss} + \mathcal{H}_c \qquad (2)$$

$$\mathcal{H}_c = \sum B_{kq} C_q^{(k)} \qquad (3)$$

where B_{kq}, in Wybourne notation, are the CF parameters and $C_q^{(k)}$ are the spherical tensor operators of Wybourne. $B_{kq} \neq 0$ in the orthorhombic symmetry crystal field only for k = 2, 4; q = 0, 2, 4. Employing SPM, the CF parameters B_{kq} are calculated [28].

The symmetry of the local field about Mn^{2+} ions in the K_2SO_4 crystal is considered to be orthorhombic (OR-type I) [5]. In OR-type I symmetry, the ZFS parameters D and E are established as follows [28]:

$$D = \left(\frac{3\varsigma^2}{70P^2D'}\right)[-B_{20}^2 - 21\varsigma B_{20} + 2B_{22}^2] + \left(\frac{\varsigma^2}{63P^2G}\right)[-5B_{40}^2 - 4B_{42}^2 + 14B_{44}^2] \qquad (4)$$

$$E = \left(\frac{\sqrt{6}\varsigma^2}{70P^2D'}\right)[2B_{20} - 21\varsigma]B_{22} + \left(\frac{\varsigma^2}{63P^2G}\right)[3\sqrt{10}B_{40} + 2\sqrt{7}B_{44}]B_{42} \qquad (5)$$

In above Eqns. P = 7B+7C, G = 10B+5C, D' = 17B+5C. B and C are Racah parameters and ς is the spin-orbit coupling parameter. With the average covalency parameter N in mind, we get $B = N^4B_0$, $C = N^4 C_0$, $\varsigma = N^2\varsigma_0$, where ς_0 presents free ion spin-orbit coupling parameter and B_0 and C_0 Racah parameters for free ion [27, 29]. For free Mn^{2+} ion, $B_0 = 960$ cm^{-1}, $C_0 = 3325$ cm^{-1} and $\varsigma_0 = 336$ cm^{-1} [5].

The parameter N is evaluated from N = ($\sqrt{B/B_0} + \sqrt{C/C_0}$)/2 taking Racah parameters (B = 850 cm^{-1}, C = 2970 cm^{-1}) obtained from optical analysis of Mn^{2+} ion in zinc cesium sulphate hexahydrate, the crystal with oxygen ligands [30], since there is no optical study of Mn^{2+} doped K_2SO_4 reported in literature.

The CF parameters, in terms of co-ordination factor $K_{kq}(\theta_j, \varphi_j)$ and intrinsic parameter $\overline{A_\kappa}(R_j)$, using SPM are found [12, 28] as

$$B_{kq} = \sum_j \overline{A_k}(R_j) K_{kq}(\theta_j, \phi_j) \quad (6)$$

$\overline{A_\kappa}(R_j)$ is provided by

$$\overline{A_k}(R_0)\left(\frac{R_0}{R_j}\right)^{t_k} = \bar{A}_k(R_j) \quad (7)$$

where the ligand's distance from the d^n ion is denoted by R_j, $\overline{A_k}(R_0)$ is the intrinsic parameter, R_0 is the reference distance of the ligand from the metal ion and t_k denotes power law exponent. For Mn^{2+}doped crystals, $t_2 = 3$ and $t_4 = 7$ are used [28]. Different values are considered in the present calculation as discussed later. As the co-ordination about Mn^{2+} ion is octahedral for all the sites, $\overline{A_4}$ is found from the relation [31]

$$\overline{A_4}(R_0) = \frac{3}{4} Dq \quad (8)$$

From optical study [30], Dq = 790 cm^{-1}. Therefore, $\overline{A_4}(R_0)$ = 592.5 cm^{-1}. For $3d^5$ ions the $\frac{\overline{A_2}}{\overline{A_4}}$ falls in the range 8 - 12 [27, 32-33]. Taking $\frac{\overline{A_2}}{\overline{A_4}}$ = 10, $\overline{A_2}$ = 5925 cm^{-1}.

IV. Results and Discussion

Using SPM, parameters $\overline{A_2}$ and $\overline{A_4}$, and the ligand arrangement about Mn^{2+} ion as indicated in Fig. 1, the CF parameters of the Mn^{2+} ion at the substitutional β-K^+ sites are computed. Table 1 provides atomic coordinates in K_2SO_4 single crystal along with bond length R (both with and without distortion) and angles θ, φ for sites I, II and III. The CF parameters using Eq. (6) and ZFS parameters from Eqs. (4) & (5) together with reference distance R_0 are depicted in Table 2. Table 2 demonstrates that R_0 = 0.200 nm is somewhat less than the sum of radii of ions (0.223 nm) of Mn^{2+} = 0.083 nm and O^{2-} = 0.140 nm along with no distortion yield ZFS parameters for substitutional octahedral site to be different from the experimental values [17]. The experimental values of ZFS parameters |D| and |E| (in 10^{-4} cm^{-1}) for sites I, II and III are 558.7, 541.9; 616.7, 522.3; 574.6, 537.2 respectively. |E|/|D| is found as 0.969, 0.846, and 0.934 being quite larger than the standard value 0.33 [25]. To have |E|/|D| in the standard range, the S4 transformation was used where the experimental |D| and |E| (in 10^{-4} cm^{-1}) become 1092.3, 8.4; 1091.7, 47.1; 1093, 18.7 with |E|/|D| 0.007, 0.043, 0.017 respectively for site I, II and III. Theoretical |E|/|D| with no distortion is also larger than the standard value 0.33 [25]. Therefore, local distortion was taken into consideration. Using above value of R_0 and local distortion, the ZFS parameters for substitutional octahedral sites I, II and III are in good accord with those from the experiment [17]. The parameters $t_2 = 3$ and $t_4 = 7$ with transformation S2 for standardization [25] have been used to obtain |E|/|D| ratio < 0.33 and calculated ZFS parameters near to experimental values.

Table 1. Atomic coordinates, bond length R (both with and without distortion), and angles θ, φ in K_2SO_4 single crystal (sites I, II and III).

Position of Mn^{2+}	Ligands	x	y	z	Spherical co-ordinates of ligands R(nm)	θ	φ°
			(Å)			θ^0	
			Without distortion				
Site : Substitutional	O1	0.250	0.417	0.048	0.10623 R_1	87.41 θ_1	90.00 φ_1
K_β	O2	0.250	-0.443	0.317	0.79618 R_2	87.72 θ_2	90.00 φ_2
(0.250, 0.317,	O3	0.037	0.347	0.317	0.26681 R_3	83.17 θ_3	94.61 φ_3
0.000)	O4	0.537	0.153	0.183	0.26916 R_4	86.10 θ_4	83.86 φ_4
	O5	-0 .037	0.847	-0.317	0.60314 R_5	93.01 θ_5	92.73 φ_5
	O6	0.463	-0.347	0.817	0.90796 R_6	84.83 θ_6	88.65 φ_6
			With distortion				
I	O1				0.18702	88.61	91.50
	O2				0.87618	89.72	92.00
	O3				0.44681	84.67	96.61
	O4				0.34916	94.10	89.86
	O5				0.78814	95.01	92.73
	O6				0.99296	86.83	90.65
II	O1				0.18704	88.61	91.50
	O2				0.87618	89.72	92.00
	O3				0.44681	84.67	96.61
	O4				0.34916	94.10	89.86
	O5				0.78814	95.01	92.73
	O6				0.99296	86.83	90.65
III	O1				0.18699	88.61	91.50
	O2				0.87618	89.72	92.00
	O3				0.44681	84.67	96.61
	O4				0.34916	94.10	89.86
	O5				0.78814	95.01	92.73
	O6				0.99296	86.83	90.65

Table 2. The Mn^{2+} doped K_2SO_4crystal's crystal field and zero field splitting parameters.

Site	CF parameters (cm^{-1}) R_0(nm)	B_{20}	B_{22}	B_{40}	B_{42}	B_{44}	ZFS parameters ($10^{-4}cm^{-1}$) |D|	|E|	|E|/|D|
				Without distortion					
Site I $\frac{A_2}{A_4}$ =10	0.200	-44451.2	-54645.9	146395.1	154947.4	209448.9	41.1	17.4	0.422
				With distortion					
Site I $\frac{A_2}{A_4}$ =10	0.200	-10081.9	8038.363	2866.375	3021.066	6400.365	1092.2	265.6	0.243
						Exp.	1092.3	8.4	0.007
Site II $\frac{A_2}{A_4}$ =10	0.200	-10079.5	8036.406	2864.366	3018.949	6397.566	1091.6	265.6	0.243
						Exp.	1091.7	47.1	0.043
Site III $\frac{A_2}{A_4}$ =10	0.200	-10085.7	8041.351	2869.444	3024.301	6404.641	1093.2	265.7	0.243

Exp.	1093.2	18.7	0.017

The CFA program [34] and B_{kq} parameters (with distortion) are used to calculate the Mn^{2+} doped K_2SO_4 single crystals' optical spectra. After diagonalization of the complete Hamiltonian, the positions of the energy bands of Mn^{2+} ion are obtained.
Table 3 displays the energy band positions for substitutional sites based on experimental and calculation data [30].

Table 3. The positions of Energy bands of single crystal of K_2SO_4 doped Mn^{2+}, both calculated and experimental.

Transition from $^6A_{1g}(S)$	Observed (cm^{-1})	Calculated (cm^{-1})		
		I	II	III
$^4T_{1g}(G)$	18436	19149, 19159, 20268, 20283, 21970, 22008	19153, 19162, 20270, 20285, 21971, 22010	19144, 19153, 20264, 20279, 21968, 22006
$^4T_{2g}(G)$	22815	22467, 22488, 23024, 23037, 23127, 23153	22469, 22490, 23025, 23038, 23128, 23155	22465, 22486, 23023, 23036, 23125, 23151
$^4E_g(G)$	24783	23457, 23472, 23662, 23685	23458, 23474, 23663, 23686	23455, 23470, 23662, 23684
$^4A_{1g}(G)$	24850	24862, 24865	24862, 24865	24862, 24865
$^4T_{2g}(D)$	28003	27347, 27365, 27835, 27851, 28972, 29045	26602, 26638, 27347, 27365, 27835, 27852	26603, 26638, 27346, 27364, 27834, 27851
$^4E_g(D)$	29870	29759, 29850, 30000, 31070	28971, 29044 29759, 29850	28975, 29048, 29759, 29850
$^4T_{1g}(P)$	32435	32351, 32434, 32829, 32935, 33089, 33244	31628, 31805, 32354, 32436, 32831, 32934	31620, 31797, 32347, 32429, 32826, 32937
$^4A_{2g}(F)$		36793, 37164	36795, 37165	36791, 37163
$^4T_{1g}(F)$	41460	40603, 41226, 41240, 41510, 41535, 41566	40603, 41226, 41240, 41509, 41534, 41567	40604, 41226, 41241, 41511, 41536, 41564

Table 3 indicates that the calculated and experimental energy band positions agree fairly well. Therefore, the theoretical results corroborate the experimental finding [17, 30] that Mn^{2+} ions enter the K_2SO_4 crystal at substitutional octahedral sites. The model parameters obtained here may be used in ZFS parameter evaluations for Mn^{2+} ions at comparable MNM sites.

V. Conclusions

Zero field splitting parameters using perturbation theory and the superposition model for K_2SO_4 single crystals doped with Mn^{2+} ions are evaluated. The ZFS parameters calculated and the experimental values agree well. The computed positions of the optical energy bands agree reasonably well with those from the experiment. Thus, experimental result is supported by the theoretical finding that Mn^{2+} ions occupy substitutional sites in K_2SO_4. The model parameters estimated in this study may be used for ZFS parameter calculations for Mn^{2+} ions at comparable locations in molecular nano magnets. The current modeling technique can be extended to explore crystals of various scientific and industrial applications.

Acknowledgement

The authors are grateful to the Head of Physics Department of Allahabad University, Allahabad for giving facilities of the department and to Prof. C. Rudowicz of Faculty of Chemistry, Adam Mickiewicz University, Poznan, Poland for CFA program.

Declarations

Ethical Approval:
This research did not contain any studies involving animal or human participants, nor did it take place on any private or protected areas. No specific permissions were required for corresponding locations.

Competing interests:

The authors declare that they have no known competing financial interests or personal relationships that could have appeared to influence the work reported in this paper.

Authors' contributions:

Maroj Bharati and Vikram Singh- performed calculations, wrote the manuscript and prepared the figure.
Ram Kripal- idea and supervision.
All authors have reviewed the manuscript.

Funding:

No funding is received.

Availability of data and materials:

The data will be made available on request.

References

[1]. J. A. Weil, J. R. Bolton, Electron Paramagnetic Resonance: Elementary Theory and Practical Applications; 2nd ed., Wiley, New York, 2007.
[2]. F. E. Mabbs, D. Collison, D. Gatteschi, Electron Paramagnetic Resonance of d Transition Metal Compounds; Elsevier, Amsterdam, 1992.
[3]. R. M. Krishna, V. P. Seth, S. K. Gupta, D. Prakash, I. Chand, J. L. Rao, EPR of Mn^{2+}-ion-doped single crystals of $Mg[C_4H_3O_4]_2{\cdot}6H_2O$, Spectrochim. Acta A **53** (1997) 253-258.
[4]. C. Rudowicz, P. Gnutek, M. Açıkg¨oz, Superposition model in electron magnetic resonance spectroscopy – a primer for experimentalists with illustrative applications and literature database, Appl. Spectrosc. Rev. 54 (2019) 673–718.
[5]. A. Abragam, B. Bleaney, Electron Paramagnetic Resonance of Transition Ion, Dover, New York, 1986.
[6]. J.R. Pilbrow, Transition-Ion Electron Paramagnetic Resonance, Clarendon Press, Oxford, 1990.
[7]. B. G. Wybourne, Spectroscopic Properties of Rare Earth, Wiley, New York, 1965.
[8]. J. Mulak, Z. Gajek, The Effective Crystal Field Potential, Elsevier, Amsterdam, 2000.
[9]. R. Bo˘ca, Zero-field splitting in metal complexes, Coord. Chem. Rev. 248 (2004) 757–815.
[10]. M. G. Brik, N. M. Avram (Eds.). Optical Properties of 3d-Ions in Crystals: Spectroscopy and Crystal Field Analysis. Heidelberg: Springer, (2013), Y. Y. Yeung: Chapter 3, pp. 95-121.
[11]. [M. G. Brik, N. M. Avram, C. N. Avram, Crystal Field Analysis of Cr^{3+} Energy Levels in $LiGa_5O_8$ Spinel, Acta Phys. Polon. A112 (2007) 1055-1060.
[12]. D. J. Newman and B. Ng, The superposition model of crystal fields, Rep. Prog. Phys. 52 (1989) 699-763.
[13]. D. J. Newman, E. Siegel**,** Superposition model analysis of Fe^{3+} and Mn^{2+} spin-Hamiltonian parameters, J. Phys. C: Solid State Phys. 9 (1976) 4285-4292.
[14]. Y. Y. Yeung, Local distortion and zero-field splittings of $3d^5$ ions in oxide crystals, J. Phys. C: Solid State Phys. 21 (1988)2453-2462.
[15]. H. Schultz, G. Bauer, E. Schachl, F. Hagedorn, P. Schmittinger, Potassium Compounds, Ullmann's Encyclopedia of Industrial Chemistry. Weinheim: Wiley-VCH. , 2005.
[16]. M. Gaultier, G. Pannetier, Structure cristalline de la forme 'basse température' du sulfate de potassium K_2SO_4-beta, Bull. Soc. Chim. France (in French), 1(1968) 105–112.
[17]. B. V. R. Chowdari, P. Venkateswarlu, Electron Paramagnetic Resonance of Mn^{2+} in K_2S0_4 Single Crystal, J. Chem. Phys. 48(1968)318-322.
[18]. W. L. Yu, M.G. Zhao, Spin-Hamiltonian parameters of ^6S state ions. Phys. Rev. B 37(1988) 9254-9267.
[19]. G. Aromí, E. K. Brechin, Synthesis of 3d metallic single-molecule magnets, Struct. Bonding 122 (2006) 1-67.
[20]. C. Coulon, H. Misayaka, R. Clérac, Single-Chain Magnets: Theoretical Approach and Experimental Systems, Struct. Bonding 122 (2006) 163-206.
[21]. M. Murrie, Cobalt(II) single-molecule magnets, Chem. Soc. Rev. 39 (2010) 1986-1995.
[22]. C. van Wüllen, Magnetic anisotropy through cooperativity in multinuclear transition metal complexes: theoretical investigation of an anisotropic exchange mechanism, Mol. Phys. 111 (2013) 2392–2397.
[23]. A. Ogg, The Crystal Structure of the Isomorphous Sulphates of Potassium, Ammonium, Rubidium, and Cesium, Phil. Mag. 5 (1928) 354-367.

[24]. C. J. Radnell, J. R. Pilbrow, S. Subramanian, M. T. Rogers, Electron paramagnetic resonance of Fe^{3+} ions in $(NH_4)_2SbF_5$. J. Chem. Phys. 62(1975) 4948-4952.

[25]. C. Rudowicz, R. Bramley, On standardization of the spin Hamiltonian and the ligand field Hamiltonian for orthorhombic symmetry. J. Chem. Phys. 83(1985) 5192- 5197.

[26]. B. N. Figgis, M. A. Hitchman, Ligand Field Theory and its Applications; Wiley, New York, 2000.

[27]. T. H. Yeom, S. H. Choh, M. L. Du, M. S. Jang, EPR study of Fe^{3+} impurities in crystalline $BiVO_4$. Phys. Rev. B 53(1996) 3415-3421.

[28]. T. H. Yeom, S. H. Choh, M. L. Du, A theoretical investigation of the zero-field splitting parameters for an Mn^{2+} centre in a $BiVO_4$ single crystal. J. Phys.: Condens. Matter 5(1993) 2017-2024.

[29]. C. K. Jorgensen, Modern Aspects of Ligand Field Theory; North- Holland, Amsterdam, 1971, p.305.

[30]. K. Purandar, J. L. Rao, S. V. J. Lakshman, Optical Absorption Spectrum of Mn2+ in Zinc Cesium Sulphte Hexahydrate, Acta Phys. Slov. 34(1984)195-207.

[31]. D. J. Newman, B. Ng (Eds.), Crystal Field Handbook; Cambridge University Press, Cambridge, 2000.

[32]. A. Edgar, Electron paramagnetic resonance studies of divalent cobalt ions in some chloride salts. J. Phys. C: Solid State Phys. 9(1976) 4303-4314.

[33]. R. Kripal, M. G. Misra, A. K. Yadav, P. Gnutek, M. Açıkgöz, C. Rudowicz, Theoretical Analysis of Crystal field Parameters and Zero field Splitting Parameters for Mn^{2+} ions in Tetramethylammonium Tetrachlorozincate, Polyhedron, 235(2023)116341.

[34]. Y. Y. Yeung, C. Rudowicz, Crystal Field Energy Levels and State Vectors for the $3d^N$ Ions at Orthorhombic or Higher Symmetry Sites. J. Comput. Phys. 109(1993) 150-152.